arXiv:1404.4159v1 [cond-mat.soft] 16 Apr 2014

Phase behaviour of two-component bottle-brush polymers with flexible backbones under poor solvent conditions

Nikolaos G Fytas[1] **and Panagiotis E Theodorakis**[2]

[1] Applied Mathematics Research Centre, Coventry University, Coventry, CV1 5FB, United Kingdom

[2] Department of Chemical Engineering, Imperial College London, London SW7 2AZ, United Kingdom

E-mail: nikolaos.fytas@coventry.ac.uk

E-mail: p.theodorakis@imperial.ac.uk

Abstract.

The phase behaviour of two-component bottle-brush polymers with fully flexible backbones under poor solvent conditions is studied via molecular-dynamics simulations, using a coarse-grained bead-spring model and side chains of up to $N = 40$ effective monomers. We consider a symmetric model where side chains of type A and B are grafted alternately onto a flexible backbone. The aim of this study to explore the phase behaviour of two-component bottle-brushes depending on parameters, such as as the grafting density σ, the backbone length N_b, the side-chain length N, and the temperature T. Based on a cluster analysis, we identify for our range of parameters the regimes of fully phase separated systems, i.e., A-type side chains form one cluster and B-type chains another, while the interface that separates these two clusters contains the backbone monomers. We find that pearl-necklace or Janus-like structures, which normally occur for bottle-brush polymers with rigid backbones under poor solvent conditions, are fully attributed to the backbone rigidity, and, therefore, such structures are unlikely in the case of bottle brushes with fully flexible backbones. Also, a comparative discussion with earlier work on the phase behaviour of single-component bottle-brush polymers with flexible backbones is performed.

PACS numbers: 02.70Ns, 64.75.Jk, 82.35.Jk

Submitted to: *Materials Research Express*

1. Introduction

Recent advances in chemical synthesis allow for the tinkering of macromolecules of complex architecture with well-defined properties, suitable for exquisite applications [1, 2]. Bottle-brush polymers are macromolecules with side chains grafted onto a backbone polymeric chain that can be intrinsically rigid or moderately flexible due to the presence of the side chains [1, 2, 3, 4, 5, 6, 7, 8, 9, 10, 11, 12, 13, 14]. The interplay between steric repulsions and effective attractions of the side-chain monomers that are grafted onto the backbone leads to intricate spatial self-organization of these macromolecules that can be tuned by variation of the solvent quality, temperature, pH, etc. [15, 16, 17, 18, 19, 20, 21]. Hence, bottle-brush polymers are stimuli responsive materials that are suitable for various applications [1, 2, 7].

Apart from synthetic bottle-brush polymers, also bio-polymers with a related architecture are abundant in nature. For instance, brush-like macromolecules that contain a protein backbone with carbohydrate side chains known as proteoglycans [22], are held responsible for a large variety of very interesting biological functions (cell signaling, cell surface protection, joint lubrication, etc.) [23, 24, 25]. In view of this interest, understanding the structure-property relation of such bottle-brush macromolecules remains a challenging problem of statistical thermodynamics due to the multitude of the involved length scales resulting from their complex structure [26, 27, 28, 29, 30, 31, 32, 33, 34, 35, 36, 37, 38, 39, 40, 41, 42, 43, 44, 45, 46, 47, 48, 49, 50, 51, 52, 53].

Nowadays, an in-depth understanding of the structural properties of bottle-brush polymers under Θ and good solvent conditions has been provided by experiment, theory and computer simulations (for instance, see the review article [6] and references therein). However, many applications require that these macromolecules exist under poor solvent conditions [7]. Apart from the experimental interest for bottle-brushes under poor solvent conditions [7], computer simulations have initially considered in their studies single-component bottle brushes under poor solvent conditions, where the backbone of the macromolecule was strictly rigid [16, 17, 19]. Moreover, theory has considered both rigid and flexible bottle-brush macromolecules [15]. For rigid backbones and when the grafting density that the side chains are grafted onto the backbone is low, the side chains do not interact with each other and collapse individually onto the rigid backbone adopting a globular conformation. As the grafting density increases to intermediate densities, side chains start to interact and clusters containing more than one side chain form pearl-necklace structures along the backbone, in line with theoretical predictions [15]. Further increase of the grafting density results in the formation of homogeneous brush cylinders [15, 16, 17, 19]. When two chemically different types of side chains are grafted alternately onto a rigid backbone, then micro-phase separation between the different monomers takes place leading to phase separation within pearls at intermediate densities [18, 19, 20]. At even higher densities, Janus-like structures are seen, where one half of the cylinder contains chains of one type and the other half side chains of the other type. The main hypothesis of this previous work has been that the

backbone is strictly rigid disregarding in this way effects due to the flexibility of the backbone.

Bottle-brush polymers with fully flexible backbones under poor solvent conditions have been only recently tackled for single-component bottle brushes [21]. In this case pearl-necklace or Janus-like structures do not occur. Therefore, such structures can only be expected for bottle brushes with non-flexible backbones. Here, we extend this work by studying the phase behaviour of two-component bottle-brush macromolecules, where two chemically different types of side chains are grafted alternately onto a flexible backbone. We focus on understanding the phase behaviour of A and B grafted chains and we make a comparison with two-component bottle brushes with rigid backbones [18, 19, 20], as well as with single-component bottle-brushes with flexible backbones [21].

The remainder of this manuscript is organized as follows: In section 2 we describe our model and sketch the analysis needed to characterize the conformations, and elucidate the phase behaviour mainly through average cluster properties. Section 3 presents our numerical results, while section 4 summarizes our conclusions.

2. Model and simulation methods

We restrict ourselves to the most symmetric case of two-component bottle-brush polymers with flexible backbones, i.e., side chains composed of different monomers denoted as A and B have the same length ($N_A = N_B = N$), with N varying within the range $N = 5 - 40$, as is done in previous works [18, 19, 20]. Although such range of chain lengths may be short to compare with theoretical predictions, we emphasize that this range of N values corresponds nicely to the lengths used in experiment [1, 2, 8, 9, 12].However, if one interprets a bead of the flexible backbones in the bead-spring model as a Kuhn segment, the simulated side groups may be longer in some of the cases studied here than in real systems with the same number of monomers per side group. Still, as an interesting theoretical, albeit academic problem, it would be nice to extend our research efforts to side-chain lengths of several hundreds of effective monomers, but this is prohibitively difficult in the poor solvent regime, where relaxation times of the chains are extremely long. The side chains are grafted regularly and alternately onto a flexible backbone with grafting density σ. There is one important distinction comparing to previous work on bottle-brushes with rigid backbones and those with flexible backbones [10, 11, 16, 17, 18, 19, 20, 21]. For bottle-brush polymers with flexible backbones the grafting density σ is quantized: we denote here by $\sigma = 1.0$ the case that every backbone monomer carries a side chain, $\sigma = 0.5$ means that every second backbone monomers has a side chain, etc. Backbone chain lengths were chosen as $N_b = 50$ and $N_b = 100$. Backbone lengths longer than $N_b = 100$ are prohibitively difficult to study. According to our previous experience, even bottle brushes in the Θ and good solvent regime [10] with longer backbone backbones are far from trivial to simulate.

We place a bottle-brush polymer in a simulation box with periodic boundary

conditions and dimensions such that no interaction of the bottle-brush polymer with its periodic images could occur. We describe both the backbone chain and the side chains by a bead-spring model [54, 55, 56], where all beads interact with a truncated and shifted Lennard-Jones (LJ) potential $U_{\rm LJ}(r)$ and nearest neighbors, bonded together along a chain, also experience the finitely extensible nonlinear elastic (FENE) potential $U_{\rm FENE}(r)$, r being the distance between the beads. Thus,

$$U_{\rm LJ}(r) = 4\epsilon_{\rm LJ}\left[\left(\frac{\sigma_{\rm LJ}}{r}\right)^{12} - \left(\frac{\sigma_{\rm LJ}}{r}\right)^{6}\right] + {\rm C}, \qquad r \leq r_c, \tag{1}$$

while $U_{\rm LJ}(r > r_c) = 0$, and $r_c = 2.5\sigma_{\rm LJ}$. The constant C is defined such that $U_{\rm LJ}(r = r_c) = 0$ is continuous at the cut-off. Henceforth, units are chosen such that $\epsilon_{\rm LJ} = 1$, $\sigma_{\rm LJ} = 1$, the Boltzmann constant $k_B = 1$, and also the mass $m_{\rm LJ}$ of all beads is chosen to be unity. When we consider two types (A, B) of side chains we still use $\sigma_{LJ}^{AA} = \sigma_{LJ}^{BB} = \sigma_{LJ}^{BB} = 1$ and $\epsilon_{LJ}^{AA} = \epsilon_{LJ}^{BB} = 1$, but $\epsilon_{LJ}^{AB} = 0.5$ to create an un-mixing tendency between A and B monomers. We know that in the case of a binary system with monomers at density $\rho = 1$ (i.e., a LJ mixture which is a standard system for the study of phase separation), macroscopic phase separation occurs below a critical temperature $T_c \approx 1.5$ [57]. For our bottle-brush polymers the average densities are much smaller, especially at distances far from the backbone, but since the critical temperature scales proportional to the chain length, we are able to detect micro-phase separation with our model. Moreover, due to the fact that the backbone is fully flexible, bottle brushes adopt globular conformations under poor solvent conditions favoring further macro-phase separation compared to bottle brushes with rigid backbones [16, 21].

The potential of equation (1) acts between any pair of beads, irrespective of whether they are bonded or not. For bonded beads also the potential $U_{\rm FENE}(r)$ acts, where

$$U_{\rm FENE}(r) = -\frac{1}{2}kr_0^2 \ln\left[1 - \left(\frac{r}{r_0}\right)^2\right] \qquad 0 < r \leq r_0, \tag{2}$$

$r_0 = 1.5$, $k = 30$, and $U_{\rm FENE}(r) = \infty$ outside the range written in equation (2). Hence r_0 is the maximal distance that bonded beads can take. Note that we did not include any explicit solvent particles; solvent-mediated interactions and solvent quality are only indirectly simulated by varying the temperature of the system as is usually done [56].

In our model the interactions of the side-chain monomers (A- and B-type) with the backbone beads (denoted with the letter C here) are the same [$\sigma_{LJ}^{\{A,B\},C} = 1.0$, $\epsilon_{LJ}^{\{A,B\},C} = 1.0$]. Hence, the influence of the backbone beads the phase behaviour of bottle-brushes is neutral, given also that all the other parameters are chosen symmetrically. This implies that, the polymer forming the backbone and the side-chain polymers on coarse-grained scale are no longer distinct. There is also no difference between the bond linking the first monomer of a side chain to a monomer of the backbone and bonds between any other pairs of bonded monomers. Of course, our attempt here does not address any effects due to a particular chemistry relating to the synthesis of these bottle-brush polymers, but, as usually done [56], we address universal features of the conformational properties of these macromolecules.

For the model defined in equations (1) and (2), the Θ temperature is known rather roughly [58], namely, $\Theta \approx 3.0$. Being interested in $T \leq \Theta$, we simulated the system for temperatures in the range $1.5 \leq T \leq 3.0$. Note however that, equilibration of collapsed chains in this temperature regime is considerably difficult, as will be discussed below. In our simulations, the temperature was controlled by the Langevin thermostat, following previous work [56, 32, 59, 60, 61, 62, 32]. The equation of motion for the coordinates $\{r_i(t)\}$ of the beads

$$m\frac{d^2\mathbf{r}_i}{dt^2} = -\nabla U_i - \gamma\frac{d\mathbf{r}_i}{dt} + \Gamma_i(t) \tag{3}$$

is numerically integrated using the GROMACS package [63, 64]. In equation (3), t denotes the time, U_i is the total potential acting on the i-th bead, γ is the friction coefficient, and $\Gamma_i(t)$ is the random force. As it is well-known, γ and Γ are related via the usual fluctuation-dissipation relation

$$< \Gamma_i(t) \cdot \Gamma_j(t^{'}) >= 6k_BT\gamma\delta_{ij}\delta(t - t^{'}). \tag{4}$$

Following references [56, 58, 32], the friction coefficient was chosen as $\gamma = 0.5$. Equation (3) was integrated with the leap-frog algorithm [65] using an integration time step of $\Delta t = 0.006\tau$, where the molecular-dynamics time unit is $\tau = (m_{\rm LJ}\sigma_{\rm LJ}^2/\epsilon_{\rm LJ})^{1/2} = 1$.

Firstly, the system was equilibrated at a temperature $T = 3.0$ using simulations extending over a time range of $30 \times 10^6\tau$. To gather proper statistics, we used 500 independent configurations at this high temperature, as initial configurations for slow cooling runs, where the temperature was lowered in steps of 0.1, and the system was simulated, at each temperature, for a time of $5 \times 10^6\tau$. The final configuration of each (higher) temperature was used as starting configuration for the next (lower) temperature. In this way, one can safely generate, at low temperatures and intermediate values of grafting densities, statistically independent configurations. Let us note here that, standard molecular-dynamics simulations would typically not sample phase space adequately at this low-temperature regime. However, this problem was overcome here by carrying out this large number of independent slow cooling runs (typically around 500 runs). The statistical accuracy of our results was also checked by varying on the same footing the cooling speed and length of runs. For temperatures above $T = 2.0$ correlations are rather insignificant, but for temperatures below $T = 2.0$ this slow cooling methodology is indispensable in order to get reliable results in our chosen range of parameters. We note that in this simulation protocol higher values of γ may be used in order to reduce the relaxation time of the chains as we are only interested for the equilibrium final states of each one of these 500 final configurations, but we decided to use the same value of γ that was introduced in the standard bead-spring model [54].

In figure 1 we show typical configurations that provide a visual overview of the phase behaviour of two-component bottle-brush polymers with flexible backbones under poor solvent conditions. At rather low temperatures far from the Θ-temperature (i.e., $T = 1.5$) the polymer collapses into a globular structure, where phase separation between

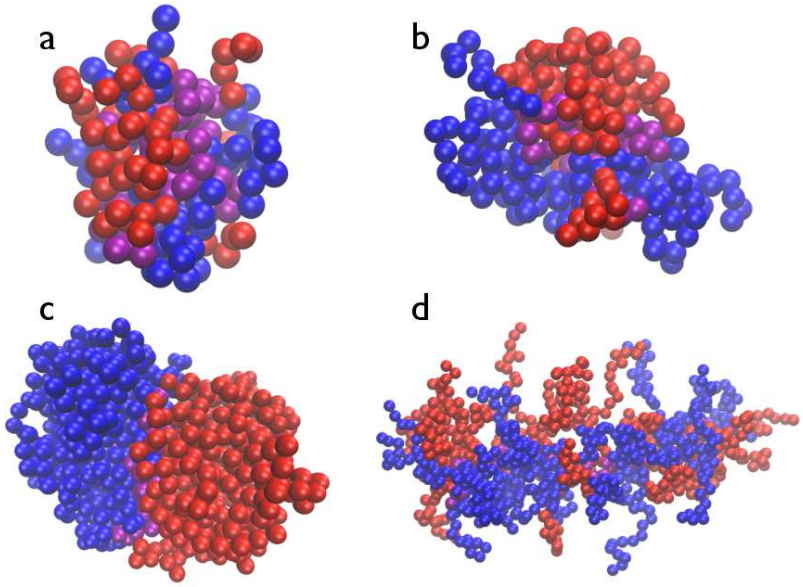

Figure 1: (Colour online) Characteristic snapshots of two component bottle-brush polymers with flexible backbones. Side chain chains of type A/B are coloured as red/blue. The backbone beads are shown in purple color. Parameters for these systems are $\sigma = 0.5$, $N_b = 50$, $T = 1.5$, and $N = 5$ (a), $N = 10$ (b) , and $N = 40$ (c). For case (d), $\sigma = 1.0$, $N_b = 50$, $N = 20$, and $T = 3.0$. In panel (a), chains A and B can not fully phase separate. In panel (b), macro-phase separation of A- and B-type of monomers occurs with a certain probability $P(N_{cl}/M)$, which is below unity. Bottle-brush polymers of case (c) are always phase separated; therefore $P(N_{cl}/M) = 1$. Panel (d) shows a snapshot at Θ temperature in the brush regime. Here, side chains of similar type are weakly correlated along the backbone resulting in unstable cluster domains of A- or B-type of chains that continuously fluctuate with regarding the number of chains that they contain.

side chains occurs only partly, figures 1(a) and (b), or fully, figure 1(c). The degree of phase separation depends strongly on the side-chain length, as well as on the grafting density. For very short side chains ($N = 5$) phase separation never takes place at a grafting density $\sigma = 0.5$, whereas for $N = 40$ macro-phase separation always occurs below a certain temperature depending on the side-chain length N, and the grafting density. As we will see below, the effect of the backbone length with respect to the phase behaviour of bottle-brush polymer can be considered as negligible.

When phase separation takes place, there is no reason a priori for the system to decide which side chains will belong to a specific cluster of the same type of monomers, also due to the symmetry of our model. We actually observe fluctuations where a side

chain of type A or B that was part of a cluster of similar monomers escapes from the cluster, to become part of another neighboring cluster with chains of the same type of monomers. Such changes in the number of chains per cluster occur rarely within the computational time limits for partly phase separated systems like the one illustrated in figure 1(b). In fact, these fluctuations are the slowest relaxation process in the system that lead to complete thermodynamic equilibrium. As discussed above, in order to achieve this equilibrium and perform a reliable statistical analysis we have used the slow cooling runs. In this way, equilibrium cluster distributions were obtained from our simulations. Without the cooling runs procedure it would be impossible to run long simulations that could be compared to the time scale of chain exchanges between clusters.

In our analysis, we distinguished between clusters of type A and B to investigate the phase separation in our model system. We remind the reader that our symmetric choice of parameters for our systems guarantee the same thermodynamic conditions for both types of chains. To analyze the clusters, we have used the Stillinger [66] neighborhood criterion for monomers: if two monomers are less than a distance r_n apart, they belong to the same cluster, where $r_n = 1.5$. Due to the symmetrically chosen set of parameters for A- and B-type of monomers, the statistical analysis for the relevant A and B clusters separately should give the same outcome. This is confirmed by our results, validating our choice of simulation procedure that allows us to obtain statistically independent configurations at sufficiently low temperatures.

3. Results and discussion

The phase behaviour of two-component bottle brushes can be analyzed through the cluster analysis discussed in the previous section. The quantity that characterizes the degree of phase separation between monomers of different type is the probability that a number of clusters per side chain occurs. Due to the symmetry of our model this probability would be equal for the two different type of chains, i.e., $P^A(N_{cl}/M) = P^B(N_{cl}/M) = P(N_{cl}/M)$. The first extreme case would be that each grafted side chain forms a separate cluster (The number of clusters N_{cl} equals the number of grafted chains A or B, i.e., $M^A = M^B = M$) with probability $P(N_{cl}/M) = 1$. In this case a side chain never forms a contact with a neighboring side chain of the same type, and the formation of clusters containing many side chains of the same type does not take place. In this case, there is no phase separation between A and B chains. The other extreme case would be that all chains are always forming one cluster probability $P(1/M) = 1$, which then corresponds to a fully phase separated system, i.e., we have one cluster of type-A chains and another cluster with type-B chains with a well defined interface between them. The backbone beads are part of this interface in a fully phase separated configuration.

In figure 2 we show the dependence of the probability $P(N_{cl}/M)$ on the side-chain length N for bottle-brushes of various grafting densities and backbone lengths. In the graphs of figure 2 we only show for clarity the lowest and the highest temperatures that

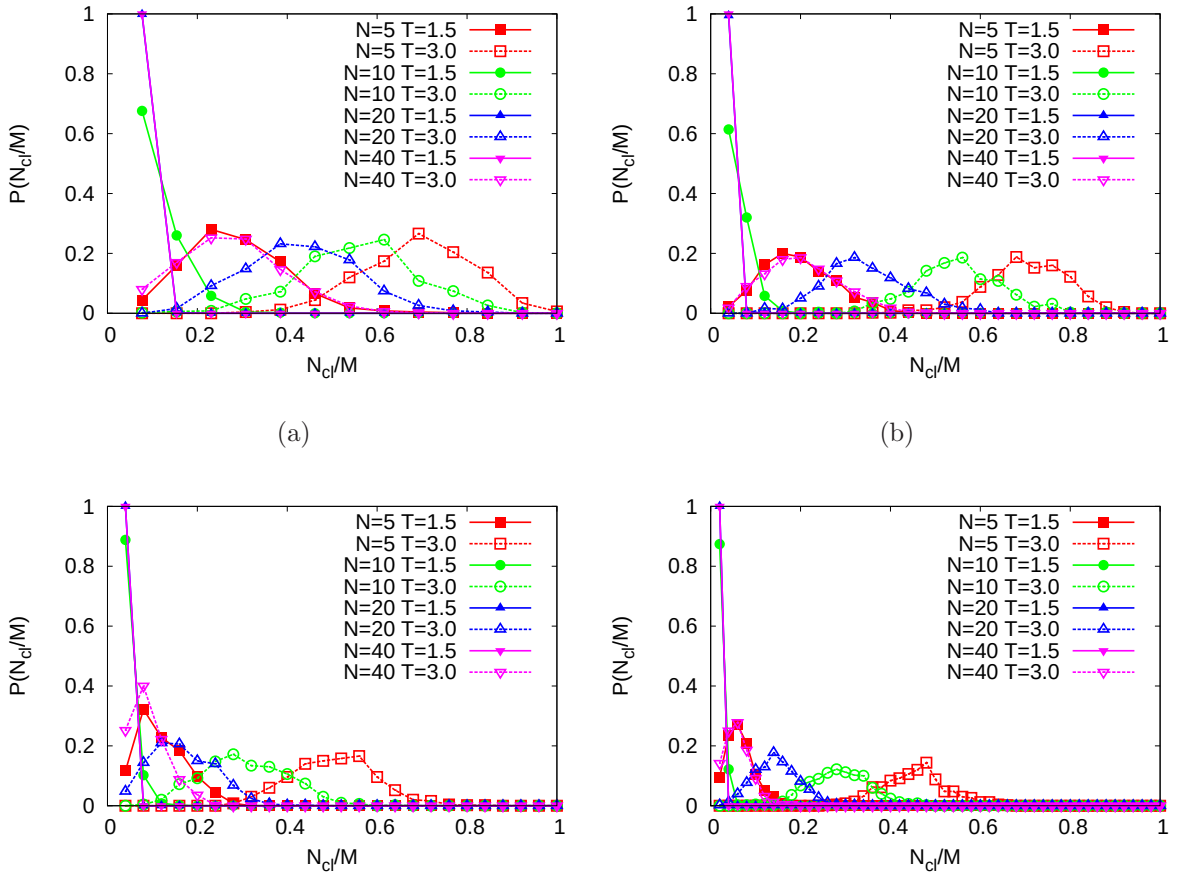

Figure 2: Probability $P(N_{cl}/M)$ that a number of clusters N_{cl} with type A or B side chains occurs. Due to the symmetry of our model the analysis of A-type clusters gives the same results as the analysis of clusters containing B-type chains. Values in the horizontal axis are normalized to the total number of grafted side chains (of type A or B) M along the backbone. In case (a) $\sigma = 0.5$ and $N_b = 50$, and the values of N and T are indicated on the graph. Similarly, in panel (b) we have $\sigma = 0.5$ and $N_b = 100$. The results of panels (a) and (b) suggest that the influence of the backbone length is negligible, while the increase of the side chain length strongly favors the phase separation of chains A from chains B. In panel (c) $\sigma = 1.00$ and $N_b = 50$, whereas in (d) $N_b = 100$. The increase in the grafting density also favors macro-phase separation between A- and B-type of side chains.

we considered in our study, namely $T = 1.5$ and $T = 3.0$. From the results of figure 2 we see that the influence of the backbone length N_b is negligible, while the grafting density σ has a rather small effect in the range considered here. The dependence on the backbone length N_b is very weak; practically, one may consider the influence due to the increase of the backbone length negligible, whereas the increase of the grafting density from $\sigma = 0.5$ to $\sigma = 1.0$ favors noticeably formation of clusters. Moreover, the distribution in the size of clusters becomes sharper as the grafting density increases showing that fluctuations in the number of clusters that build the cluster aggregations are becoming suppressed. In figure 2, we can also see that complete phase separation between A and B chains for bottle-brushes with small side chains ($N = 5$) is rarely possible at high grafting densities. For $N = 10$, phase separation between A- and B-type of monomers occurs with probability around 60% for $\sigma = 0.5$ and about 80% for $\sigma = 1.0$ for the lowest temperature ($T = 1.5$). For side-chain lengths longer than $N = 10$, monomers A and B are always phase separated. At temperatures close to the Θ ($T = 3.0$) the formation of clusters with A chains and clusters with B chains is still possible even for short chain lengths. Finally, the increase of the grafting density clearly favors the formation of clusters at every temperature between $T = 1.5$ and $T = 3.0$ as we will also discuss more in detail below.

In figure 3 we illustrate the dependence of the cluster formations on the temperature for four characteristic cases. In figure 3(a) no macro-phase separation takes place for the whole range of temperatures between $T = 1.5$ and $T = 3.0$ ($\sigma = 0.5$ and $N_b = 100$). As the temperature decreases the formation of clusters is favored. Despite the short length of the side chains, small clusters containing a few side chains are possible even at $T = 3.0$. When the side-chain length increases [figure 3(b)], i.e., $N = 40$, macro-phase separation is already initiated at temperature $T = 2.7$. Moreover, at temperatures below $T = 2.1$ a cluster containing all side chains of type A and another cluster containing all side chains of type B is formed, with a well-defined interface between them that contains the backbone monomers. When the grafting density increases [figures 3(c) and (d)], macro-phase separation is favored at all temperatures. For $N = 5$, figure 3(c), macro-phase separation occurs with a small probability for $\sigma = 1.0$, whereas never occurred for $\sigma = 0.5$. The same is true for $N = 40$, comparing figures 3(b) and (d). By examining all the cases studied here, we found that at temperature $T = 3.0$, no macro-phase separation occurs for any of our cases; as expected phase separation is initiated at temperatures below the Θ temperature as a result of the favoring attractions between beads of the same type.

Although the results of figures 2 and 3 clearly provide an overview of the phase behaviour of bottle-brush macromolecules with flexible backbones for the current range of parameters, little information is provided on the interface between phase separated systems. Therefore, we have also measured the number of unfavorable contacts n_{AB} for

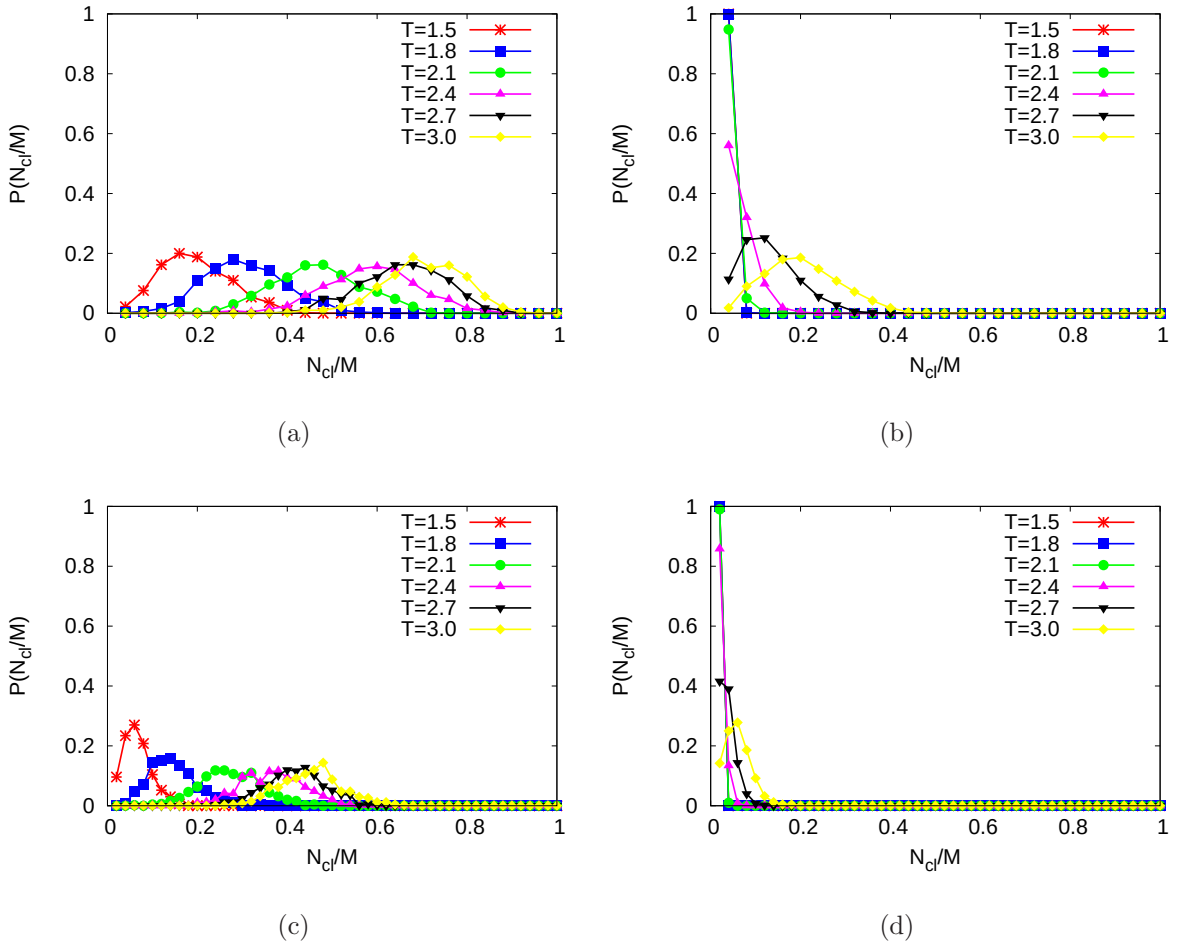

Figure 3: The dependence of the probability $P(N_{cl}/M)$ on the temperature T is shown for four characteristic cases (a)-(d). We start with panel (a) where $\sigma = 0.5$, $N_b = 100$, and $N = 5$. For the range of temperatures $T = 1.5$ to $T = 3.0$ clusters containing a few side chains are formed. The chains that are part of a cluster can leave one cluster and become part of another. The cluster sizes are distributed symmetrically around an average value, as in figure 2. In this case, the grafting density and the side-chain length are not high enough to lead to a fully phase-separated system, where side-chains of type A are part of single cluster and those of type B of another. In panel (b), $\sigma = 0.5$, $N_b = 100$, and $N = 40$. Here the side-chain length is high enough to lead to a fully phase separated system for temperatures $T < 2.1$. A small variation in the number of clusters is observed for the rest of the temperatures shown. Panel (c) presents results for the case $\sigma = 1.0$, $N_b = 100$, and $N = 5$. Increase in the grafting density from $\sigma = 0.5$ to $\sigma = 1.0$ occasionally leads to a fully macro-phase separated system at temperature $T = 1.5$, although the side-chain length is still short. Finally, panel (d) refers to the parameters $\sigma = 1.0$, $N_b = 100$, and $N = 40$. Here, chains of A- and B-type are for all configurational samples fully separated at temperatures $T < 2.4$.

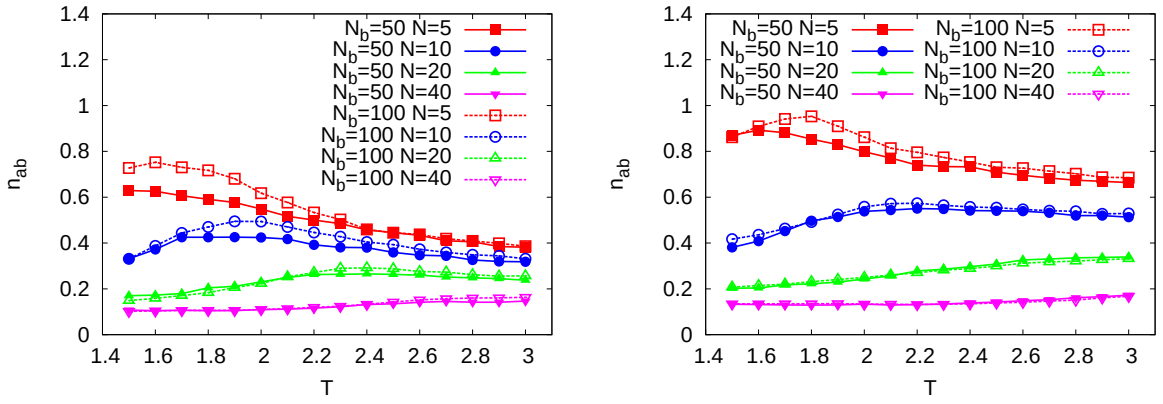

(a) (b)

Figure 4: The number of unfavourable contacts, i.e., the number of contacts between A- and B-type monomers, as a function of temperature for various bottle-brush polymers, as indicated on the graphs. In panel (a) $\sigma = 0.5$, while in panel (b) $\sigma = 1.0$. The different behaviour shown here is attributed to the presence of the interface between A and B side chains in a fully phase separated system [see, i.e., figure 1(c)]. For more details, we refer to the discussion in the main body of the text.

our systems which is expressed by the following formula

$$n_{AB} = 4\pi \int_0^{r_n} g_{AB}(\Delta r)(\Delta r)^2 d(\Delta r), \tag{5}$$

where Δr is the absolute value of the distance between two sites of monomers at positions $\vec{r}_i, \vec{r}_j$, and g_{AB} the corresponding radial distribution function. Equation (5) means that a pair of monomers (A, B) is defined to have a pairwise contact if their distance is less than r_n.

Figure 4(a) presents the average contacts per monomer between monomers of A- and B-type for bottle brushes with grafting density $\sigma = 0.5$, whereas the results presented in figure 4(b) correspond to the case $\sigma = 1.0$. The results of figures 2 and 3 help us interpret those of figure 4, because they sketch the phase behaviour of our systems. Overall, the increase of the grafting density leads to a relevant increase in the number of contacts. For both grafting densities $\sigma = 0.5$ and $\sigma = 1.0$ we can distinguish three cases. In the first case, the bottle-brush polymers with very short chains ($N = 5$) and lower grafting density ($\sigma = 0.5$) belong; here, macro-phase separation does not take place and a well-defined interface between A- and B-type monomers is not present. For this case a monotonic decrease in the number of unfavorable contacts n_{AB} occurs. At low temperatures, where the bottle-brush has a globular structure, the increase of the backbone length results in higher number of contacts between A and B, which is a direct consequence of the increase in the number of grafted side chains.

The second case corresponds to bottle-brush polymers for which at lower

temperatures only two clusters of A or B chains are always fully separated with a well-defined interface, and at higher temperature more clusters of A or B chains exist. At lower temperatures an increase of n_{AB} with the increase in temperature is seen, as the attraction between beads of the same type weakens and A- and B-type of monomers approach the interface. At higher temperatures, the number of unfavorable contacts n_{AB} decreases with an increase in the temperature. Therefore, the change in the slope as the temperature increases from lower to higher temperatures signals the change in the phase behaviour of the system and the disappearance of the well-defined A-B interface between A and B chains.

The third case we could identify from the graphs of figure 4 corresponds to a "strong" macro-phase separation between A- and B-type of monomers for a large range of temperatures. These are cases that are related to bottle-brush polymers with high grafting density and, more importantly, long side chains. Here, the number of unfavorable contacts n_{AB} shows a monotonic increase with the increase of the temperature. For relatively long side chains phase separation between individual chains becomes strong and an interface between individual chains is possible at temperatures below the Θ temperature. Therefore, we see a considerable change in behaviour between bottle-brushes with short side chains and bottle-brushes with long side chains. In the latter case, phase separation between individual grafted chains becomes pronounced.

The above analysis of the unfavorable contacts provide some clue for the presence of a well-defined interface between A and B chains. However, we could gain additional insight in the overall picture of the bottle brushes examined in this work by computing the averaged overall density of monomers, which is mathematically expressed by the following formula

$$\rho(|\vec{r}|) = \langle \sum_{i=1}^{nN} \delta(\vec{r} - \vec{r}_c - \vec{r}_i) \rangle. \tag{6}$$

In the above equation $\delta(\vec{x})$ is the Dirac delta function, $\vec{r}_c$ is the position of the center of mass of all monomers that belong to the chain, and $\vec{r}_i$ are the positions of all monomers, irrespective of whether they belong to the backbone or to the side chains, and also irrespective of whether they are of A or B type. The angle brackets denote an average over all conformations, as usual.

Figure 5 shows three characteristic examples of the overall monomer density for different choices of parameters σ, N_B, and N, and for three different temperatures only chose for clarity. Cases on each graph of figure 5 correspond to two different bottle-brushes that contain the same total number of monomers. For example, figure 5(b) presents results for one bottle brush with parameters $\sigma = 0.5$, $N_b = 100$, and $N = 20$, and another with parameters $\sigma = 1.0$, $N_b = 100$, and $N = 10$. Similarly are chosen the parameters for graphs (a) and (c) of figure 5. From the figures we can see that the overall monomer distribution of the monomers for macro-phase separated systems at temperature $T = 1.5$ is similar for different bottle brushes with the same total number of monomers. Therefore, it is not possible to verify from this property the presence of

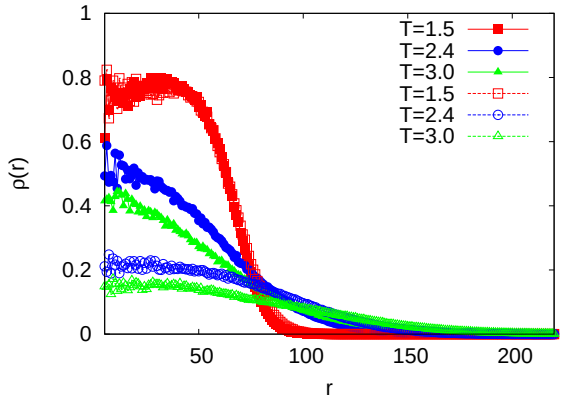

(a)

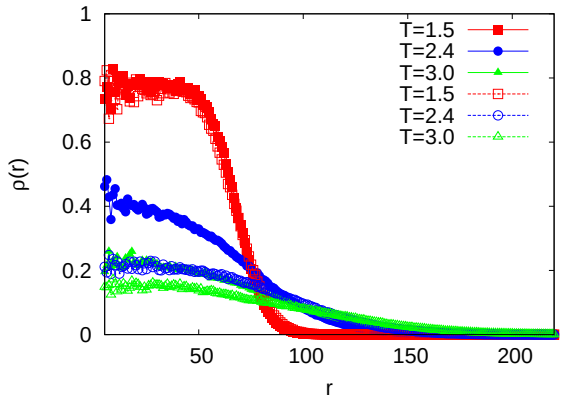

(b)

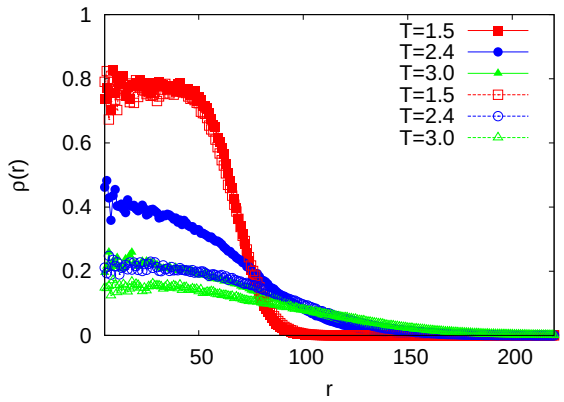

(c)

Figure 5: Density profiles $\rho(r) = \rho(|\vec{r}|)$ plotted versus the radial distance $r = |\vec{r}|$ from the center of mass of the bottle-brush. Various temperatures are shown as indicated. Case (a) presents results for bottle-brush polymers with $\sigma = 1.0$, $N_b = 50$, and $N = 20$ (full symbols) and $\sigma = 1.0$, $N_b = 100$, and $N = 10$ (open symbols). In graph (b) results refer to bottle-brush macromolecules with $\sigma = 0.5$, $N_b = 100$, and $N = 20$ (full symbols) and $\sigma = 1.0$, $N_b = 100$, and $N = 10$ (open symbols). Panel (c) refers to $\sigma = 0.5$, $N_b = 100$, and $N = 40$ (full symbols), and $\sigma = 1.0$, $N_b = 100$, and $N = 20$ (open symbols). Whereas in the case of multi-block copolymers the interface of a macro-phase separated system can be easily detected through averaged overall profiles [59, 61],

a well-defined interface between A- and B-type of monomers. At higher temperatures ($T = 2.4$ and $T = 3.0$) more pronounced differences are observed in the density profiles of the bottle- brushes depending on the grafting density σ and the side-chain length N. Examination of the profiles of figure 5 can also provide further information on the transition of a globular structure at low temperatures to a bottle-brush-like structure at higher temperatures, i.e., temperatures close to the Θ temperature. The apparent similarities in the density profiles and the fact that the interface A-B does not play such a significant role as for other polymer macromolecules of complex architecture (e.g., multi-block co-polymers [59, 60, 61, 62]) may suggest that the conformational properties of two-component bottle-brushes (e.g. mean square gyration radius of side chains, etc.) may not differ significantly from the corresponding properties for single-component bottle-brushes with flexible backbones [21].

4. Conclusions

Prior work on bottle-brush polymers has documented the phase behaviour of bottle brushes with rigid backbones under poor solvent conditions. It was found that for intermediate and high grafting densities, pearl-necklace and Janus-like structures are formed. In the present contribution, we discussed the phase behaviour of two-component bottle-brush polymers with flexible backbones under poor solvent conditions, by means of extensive molecular-dynamics simulations.

For our range of parameters that can be directly compared to bottle-brushes with a rigid backbone of previous studies [18], we found that the formation of pearl-necklace or Janus-like structures does not take place when the backbone is fully flexible. Therefore, the aforementioned structures are totally attributed to the rigidity of the backbone. When the grafting density, or the side-chain length, increases, phase separation is favoured, indeed. The backbone length seems to play no role for the range of parameters examined here. Our findings extend previous work on bottle-brush polymers with rigid backbones [18] and provide an outline on the phase behaviour of two-component bottle-brush polymers, since the fully flexible and rigid backbone cases are the two limiting cases for this type of complex systems.

Thus far, all simulation studies have been realized for rather moderate chain lengths, which, however, serve our current needs for comparison with experimental work. As a future challenge, it would be favourable to have numerical data for larger systems, although this task is currently hindered by the huge relaxation times of such macromolecules at low temperatures. Finally, it is worth noting that a more detailed study for intermediate rigidities that may reveal interesting structures would be desirable, serving as a bridge between the current and previous works [17, 18].

References

[1] Zhang M and Müller A H E 2005 *J. Polym. Sci.* **43** 3461

[2] Sheiko S S, Sumerlin B S and Matyjaszewski K 2008 *Prog. Polym. Sci.* **33** 759
[3] Maleki H and Theodorakis P E 2011 *J. Phys.: Condens. Matter* **23** 505104
[4] Subbotin A V and Semenov A N 2007 *Polym. Sci.* bf 49 1328
[5] Potemkin I I and Palyulin V V 2009 *Polym. Sci.* **51** 123
[6] Binder K and Milchev A 2012 *J. Polym. Sci.* **50** 1515
[7] Walther A and Müller A H E 2013 *Chem. Rev.* **113** 5194
[8] Rathgeber S, Pakula T, Matyjaszewski K and Beers K L 2005 *J. Chem. Phys.* **122** 124904
[9] Zhang B, Gröhn F, Pedersen J S, Fischer K and Schmidt M 2006 *Macromolecules* **39** 8440
[10] Theodorakis P E, Hsu H-P, Paul W and Binder K 2011 *J. Chem. Phys.* **135** 164903
[11] Theodorakis P E and Fytas N G 2012 *Am. J. Condens. Matter Phys.* **2** 101
[12] Hsu H-P, Paul W and Binder K 2010 *Macromolecules* **43** 3094
[13] Feuz L, Strunz P, Geue T, Textor M and Borisov O 2007 *Eur. Phys. J E.* **23** 237
[14] Lee H I, Matyjaszewski K, Yu-Su S and Sheiko S S 2008 *Macromolecules* **41** 6073
[15] Sheiko S S, Borisov O V, Prokhorova S A and Möller M 2004 *Eur. Phys. J. E* **13** 125
[16] Theodorakis P E, Paul W and Binder K 2009 *Europhys. Lett.* **88** 63002
[17] Theodorakis P E, Paul W and Binder K 2010 *J. Chem. Phys.* **133** 104901
[18] Theodorakis P E, Paul W and Binder K 2011 *Eur. Phys. J. E* **34** 52
[19] Erukhimovich I, Theodorakis P E, Paul W and BinderK 2011 *J. Chem. Phys.* **134** 054906
[20] Theodorakis P E, Paul W and Binder K 2010 *Macromolecules* **46** 5137
[21] Fytas N G and Theodorakis P E 2013 *Journal of Phys.: Condens. Matter* **25** 285105
[22] Iozzo R V (Editor) 2000 *Proteoglycans: Structure, Biology and Molecular Interactions* (Marcel Dekker: New York)
[23] Muir H 1983 *Biochem. Soc. Trans.* **11** 613
[24] Kaneider N C, Dunzendorfer S and Wiedermann C J 2004 *Biochemistry* **43** 237
[25] Klein J 2009 *Science* **323** 47
[26] Birshtein T M and Zhulina E B 1984 *Polymer* **25** 1453
[27] Witten T A and Pincus P A 1986 *Macromolecules* **19** 2509
[28] Birshtein T M, Borisov O V, Zhulina E B, Khokhlov A R and Yurosowa T A 1987 *Polym. Sci. U.S.S.R.* **29** 1293
[29] Wang Z G and Safran S A 1988 *J. Chem. Phys.* **89** 5323
[30] Ligoure C and Leibler L 1990 *Macromolecules* **23** 5044
[31] Ball R C, Marko J F, Milner S T and Witten T A 1991 *Macromolecules* **24** 69
[32] Murat M and Grest G S 1991 *Macromolecules* **24** 704
[33] Dan N and Tirrell M 1992 *Macromolecules* **25** 2980
[34] Jijmans C M and Zhulina E B 1993 *Macromolecules* **26** 7214
[35] Fredrickson G H 1993 *Macromolecules* **26** 2825
[36] Li H and Witten T A 1994 *Macromolecules* **27** 449
[37] Rouault Y and Borisov O V 1996 *Macromolecules* **29** 2605
[38] Sevick E M 1996 *Macromolecules* **29** 6952
[39] Saariaho M, Ikkala O, Szleifer I, Erukhimovich I and ten Brinke G 1997 *J. Chem. Phys.* **107** 3267
[40] Saariaho M, Szleifer I, Ikkala O and ten Brinke G 1998 *Macromol. Theory Simul.* **7** 211
[41] Rouault Y 1998 *Macromol. Theory Simul.* **7** 359
[42] Saariaho M, Subbotin A, Szleifer I, Ikkala O and ten Brinke G 1999 *Macromolecules* **32** 4439
[43] Shiokawa K, Itoh K and Nemoto M 1999 *J. Chem. Phys.* **111** 8165
[44] Subbotin A, Saariaho M, Ikkala M and ten Brinke G 2000 *Macromolecules* **33** 3447
[45] Khalatur P G, Shirvanyanz D G, Staravoitova N Y and Khokhlov A R 2000 *Macromol. Theory Simul.* **9** 141
[46] Stepanyan R, Subbotin A and ten Brinke G 2002 *Macromolecules* **35** 5640
[47] de Jong J and ten Brinke G 2004 *Macromol. Theory Simul.* **13** 318
[48] Elli D, Ganazzoli F, Timoshenko E G, Kuznetsov Y A and Connolly R 2004 *J. Chem. Phys.* **120** 6257

[49] Connolly R, Bellesia G, Timoshenko E G, Kuznetsov Y A, Elli S and Ganazzoli F 2005 *Macromolecules* **38** 5288
[50] Yethiraj A 2005 *J. Chem. Phys.* **125** 204901
[51] Chang R, Kwak Y and Gebremichael Y 2009 *J. Mol. Biol.* **39** 648
[52] Hsu H-P, Paul W and Binder K 2007 *Macromol. Theory Simul.* **16** 660
[53] Hsu H-P, Paul W and Binder K 2008 *J. Chem. Phys.* **129** 204904
[54] Grest G S and Kremer K 1986 *Phys. Rev. A* **33** 3628
[55] Murat M and Grest G S 1989 *Macromolecules* **22** 4054
[56] Binder K 1995 *Monte Carlo and Molecular Dynamics Simulations in Polymer Science* (Oxford University Press: New York)
[57] Das S K, Horbach J and Binder K 2003 *J. Chem. Phys.* **119** 1547
[58] Grest G S and Murat M 1993 *Macromolecules* **26** 3108
[59] Theodorakis P E and Fytas N G 2011 *Soft Matter* **7** 1038
[60] Theodorakis P E and Fytas N G 2011 *Europhys. Lett.* **93** 43001
[61] Fytas N G and Theodorakis 2011 *J. Phys.: Condens. Matter* **23** 235106
[62] Theodorakis P E and Fytas N G 2012 *J. Chem. Phys.* **136** 094902
[63] Berendsen H J C, van der Spoel D and van Drunen R 1995 *Comp. Phys. Comm.* **19** 43
[64] Lindahl E, Hess B and van der Spoel D 2001 *Mol. Mod.* **7** 306
[65] van Gunsteren W F and Berendsen H J C 1988 *Mol. Simul.* **1** 173
[66] Stillinger F H 1963 *J. Chem. Phys.* **38** 1486

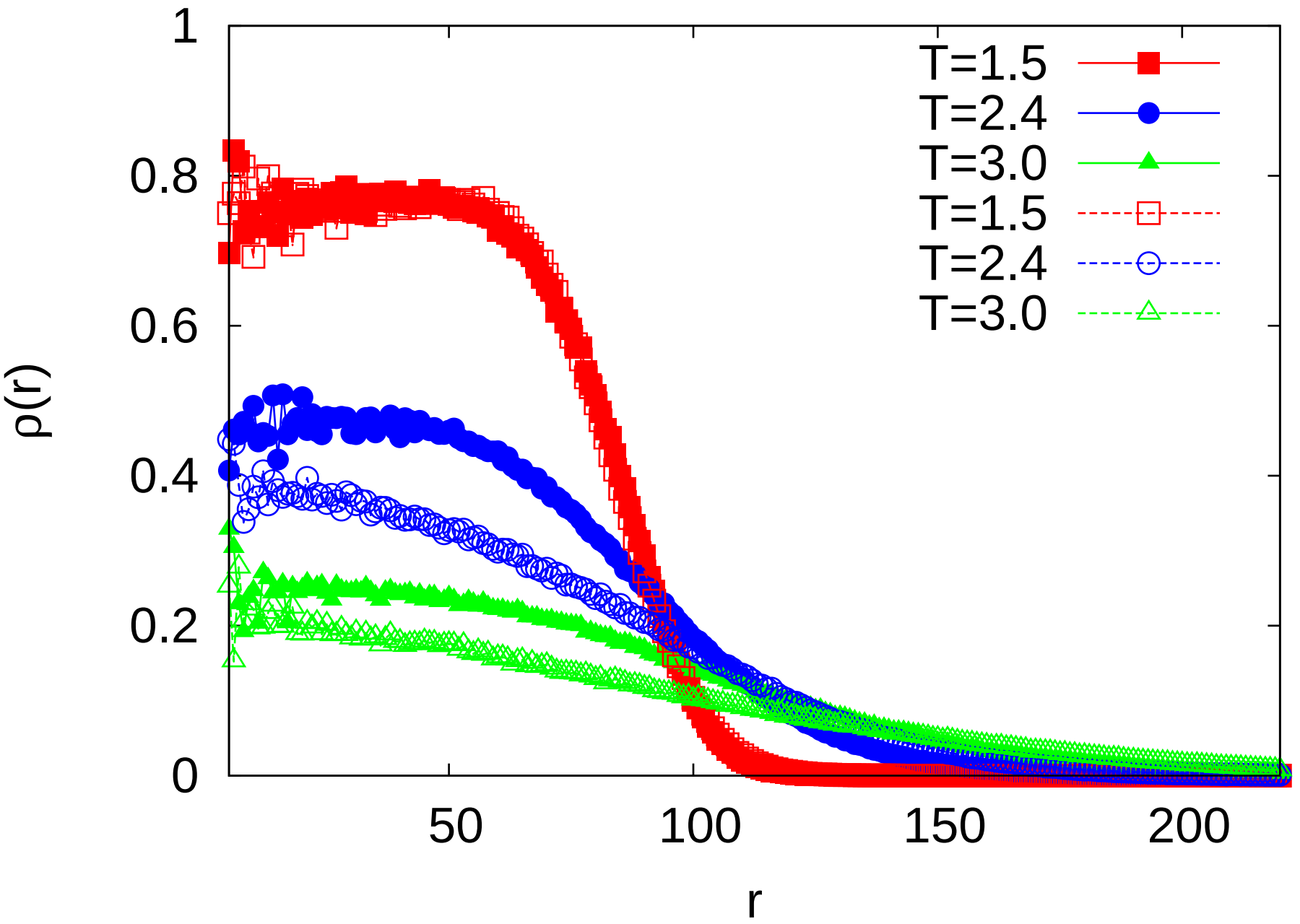
1
0.8
0.6
0.4
0.2
0
p(r)
50
100
150
200
r
T=1.5
T=2.4
T=3.0
T=1.5
T=2.4
T=3.0